A Comparison of Robust and Probabilistic Reliability for Systems with Renewables and Responsive Demand

Jialin Liu*, Gabriela Martínez*, Bowen Li†, Johanna Mathieu†, C. Lindsay Anderson*
*Cornell University, {jl3455,mgm256,cla28}@cornell.edu
† University of Michigan, {libowen,jlmath}@umich.edu

***Abstract*—The effective integration of significant levels of intermittent renewable resources in power system operations will be enabled by increased participation of demand-side resources. In this work, the use of these demand-side resources for balancing reserves is examined in the context of solutions with varying degrees of robustness. The objective is a simulation-based analysis of the impact of requiring robust versus non-robust solutions, the latter in the form of chance-constrained solutions. We use a stochastic optimal power flow formulation that leverages various classes of reserves, from both generation and responsive demand, to manage considerable uncertainty in renewable generation. Case studies with a 30-bus system illustrate that reserve allocations under the robust formulation, though reliable, may cause undue stress to the system that could render the dispatch implementation infeasible. Conversely, the flexibility introduced in a chance-constrained formulation, even at risk-averse probability levels, produces more realistic allocations of generation and reserves, and can be adjusted to provide full robustness at critical, or highly uncertain, periods in the planning horizon. This flexibility is advantageous to the system and customizable by the operator.**

***Keywords*-renewable energy, chance constraints, responsive demand, optimal power flow**

I. Introduction

The undeniable benefits of renewable energy sources are inspiring increasing investment in these technologies. In conjunction with the environmental and economic benefits of renewable energy, the most common renewable sources, such as wind and solar, also increase uncertainty in power system operation and planning. In answer to increasing uncertainty, the development of stochastic methods for system operations has been an active area of research. Stochastic methods for power system operations are being developed for security constrained unit commitment (SCUC), and the optimal power flow problem (OPF), both of which must be updated to account for uncertainty.

The approaches taken to both of these applications can be broadly categorized into three classes: scenario-based stochastic programming, robust optimization methods, and probabilistic optimization. Scenario-based stochastic programming approaches have been widely used for both UC and OPF, wherein the decision maker determines the set of possible scenarios, and the solution to the optimization model will provide a minimum expected cost solution based on probability weighted scenarios, for example [1]–[3]. The two primary challenges of stochastic programming methods are 1) the implicit assumption that all credible future scenarios are included, and 2) the computational challenge of the optimization algorithm with a reasonable set of scenarios. In answer to these challenges, and in line with traditional requirement for reliability at all costs, robust optimization methods have been gaining popularity. Robust optimization methods are designed to provide solutions that are cost minimizing under the worst possible future outcome, where uncertainty is often characterized by assumed underlying distributions [4], [5] that may be non-stationary over a rolling horizon [6]. Under the assumption that future uncertainty is well-represented by the underlying distributional assumptions, robust methods provide secure solutions, with computational tractability. However, these solutions will provide an upper bound on solution cost that may be exceedingly restrictive in their use of renewable resources [7]. A compromise between stochastic programming and robust methods is probabilistic (chance-constrained) optimization, which allows constraint violation with very low probability. The advantage of this method is greater flexibility in solutions, allowing more or less "robustness" across space and time according to the needs or knowledge of the system operator [8]–[12]. The primary goal of all of these methods is the most cost effective and reliable allocation of available units, generation, and reserves.

The current level of wind generation in the US power system is such that the uncertainty introduced can be managed via ramping and reserves provided by other generators within the system. At greater levels of wind penetration, these reserves may be unavailable or not economically viable, and the industry is actively investigating alternative strategies to ensure reliability [13]–[15]. The most daunting challenges of the transformation of the power system arise from the timescale for implementation, and the prohibitive cost of solutions like additional fast-ramping generation or

This work was supported in part by the Consortium for Electric Reliability Technology Solutions and the Office of Electricity Delivery and Energy Reliability, Transmission Reliability Program of the U.S. Department of Energy, and NSF Grant #CCF-1442495.

grid-scale storage. The promise of demand-side resources in this arena lies in the spatially widespread availability, rapid response, and lower cost of using resources that already exist in the system [16]. However, the challenge of responsive demand arises from the need to understand, manage, and incent a very large number of resources to participate effectively toward serving the objective of the power system [17]. The inclusion of responsive demand in the operational models such as SCUC and OPF, will allow endogenous determination of the best use of these, and other, reserve resources to maintain system reliability, make effective use of available renewables, and keep system costs within reasonable bounds.

This work builds on the approach of [11], which uses a chance-constrained formulation to determine reserve allocations among generators and responsive loads, accounting for uncertainty in wind and responsive demand. The model described in [11] is augmented here with significant wind capacity over multiple wind farms, and a realistic forecast model featuring increasing forecast error over the planning horizon. Additionally, we explore the impact of varying the risk-level of the probabilistic constraints to require more robust solutions when uncertainty is significant, as described in [10]. Previous work has not specifically considered the use of customized risk levels to manage critical time periods, nor the trade-off between robustness and feasibility. Within this framework, we conduct a simulation-based analysis to compare the solutions obtained using both the robust and the chance-constrained approaches applied to a 30-bus system. In Section II we describe the formulation of the model. In Section III, the numerical results are presented in the context of the test cases, and concluding remarks are in included Section IV.

II. Model Formulation

The framework used here includes thermostatically controlled loads (TCLs) as a reserve resource in an optimal power flow model, following the approach described in [11]. Loads and generators provide secondary reserves to adjust for errors in the wind generation forecast, and generators are re-dispatched every 15 minutes to manage the energy state of the loads. The model described in [11] is implemented with the following modifications: 1) a deterministic temperature profile is used so that load-based reserve capacities are certain; 2) the generation and load schedule are functions of the expected variability of wind generation at high penetration levels (specifically, through the inclusion of four wind farms in a 30-bus network); and 3) the hour-to-hour coupling constraints formulated in [11] are eliminated because they are conservative and removing them reduces computational effort. For completeness, we provide a very generalized description of the model below, and the reader is directed to [11] for the detailed formulation.

A. Nomenclature

- $\mathcal{C}^{\text{det}}$ deterministic constraints on generators, flows, loads, and storage
- $\mathcal{C}_{GD}$ probabilistic constraints associated with the re-dispatch reserves from generators
- $\mathcal{C}_{GS}$ probabilistic constraints associated with the secondary reserves from generators
- $\mathcal{C}_{LS}$ probabilistic constraints associated with the secondary reserves from controllable loads
- $\mathcal{C}^{\text{load}}_{\text{dyn}}$ probabilistic dynamic controllable load constraints
- ϵ constraint violation probability
- $\overline{P}_C(\mathcal{T}_t)$ controllable load power upper bound vector in period t at temperature $\mathcal{T}$
- $\overline{S}(\mathcal{T}_t)$ controllable load energy state upper bound vector in period t at temperature $\mathcal{T}$
- $\underline{P}_C(\mathcal{T}_t)$ controllable load power lower bound vector in period t at temperature $\mathcal{T}$
- C_n cost function of the generators
- C_{GD} cost function of the re-dispatch reserves from generators
- C_{GS} cost function of the secondary reserves from generators
- C_{LS} cost function of the secondary reserves from controllable loads
- $d^{1,up/dn}_{GD,t}$ generator upward/downward re-dispatch reserve distribution vector for wind forecast error in period t
- $d^{2,up/dn}_{GD,t}$ generator upward/downward re-dispatch reserve distribution vector for restoring controllable load energy state in period t
- $d^{up/dn}_{GS,t}$ generator upward/downward secondary reserve distribution vector in period t
- $d^{up/dn}_{LS,t}$ controllable load upward/downward secondary reserve distribution vector in period t
- $P_B(\mathcal{T}_t)$ controllable load baseline power vector in period t at temperature $\mathcal{T}$
- $P_{C,t}$ controllable load power set point vector in period t
- $P_{G,t}$ generator generation vector in period t
- $R^{up/dn}_{GD,t}$ generator upward/downward re-dispatch reserve capacity vector in period t
- $R^{up/dn}_{GS,t}$ generator upward/downward secondary reserve capacity vector in period t
- $R_{LS,t}$ actual controllable load secondary reserve vector in period t
- $R^{up/dn}_{LS,t}$ controllable load upward/downward secondary reserve capacity vector in period t
- S_t controllable load energy state vector

B. Demand Response Model

The demand response model exploits the potential of TCLs, such as air conditioners (ACs), to provide ancillary services to balance generation and demand. Aggregations of TCLs are modeled as time-varying thermal energy storage devices [18] and their power consumption $P_{C,t}$ is controlled externally by a load aggregator, where t is the time index. Control actions are assumed to be non-disruptive [17], specifically all conditioned spaces stay within a narrow ($\sim$ 1°C) temperature range around their temperature set point. A baseline $P_B(\mathcal{T}_t)$ is used to represent the power consumption of an aggregation of TCLs under its own internal control, and it is a function of ambient temperature $\mathcal{T}_t$. External control influences the aggregation's thermal energy state S_t as follows:

$$S_{t+\Delta\tau} = S_t + (P_{C,t} - P_B(\mathcal{T}_t))\Delta\tau \tag{1}$$

$$0 \leq S_t \leq \overline{S}(\mathcal{T}_t), \tag{2}$$

$$\underline{P}_C(\mathcal{T}_t) \leq P_{C,t} \leq \overline{P}_C(\mathcal{T}_t), \tag{3}$$

where $\Delta\tau$ is the time step. The power capacity $[\underline{P}_C(\mathcal{T}_t), \overline{P}_C(\mathcal{T}_t)]$ represents the range of real time power output from the load aggregation. The energy capacity $[0, \overline{S}(\mathcal{T}_t)]$ represents the range of its energy state. Both ranges are bounded and calculated with the method described in [18].

C. Day-ahead Optimal Dispatch Model

The linearized power flow model (usually referred to as the DC power flow model) is used to obtain the optimal dispatch. The system has two classes of reserves: 1) secondary frequency control from generators and loads denoted R_{GS} and R_{LS}, respectively, and 2) intra-hour re-dispatch from the generators, denoted R_{GD}.

Following [8], [9], let d_{GS} and d_{LS} be the generator and load secondary frequency control "distribution vectors," which distribute the wind forecast error to different generation and load units. Wind forecast errors are compensated for by secondary frequency control, and re-dispatch is activated every 15 minutes to 1) compensate the intra-hour wind forecast error, which is managed by a distribution vector d^1_{GD}, and 2) restore the energy state of the TCLs, which is managed by a distribution vector d^2_{GD}. The optimization model decides the day-ahead dispatch for the following decision variables:

$$\begin{aligned} x_t = [&P_{G,t}, P_{C,t}, R^{up}_{GS,t}, R^{dn}_{GS,t}, R^{up}_{LS,t}, R^{dn}_{LS,t}, R^{up}_{GD,t}, R^{dn}_{GD,t},\\ &d^{up}_{GS,t}, d^{dn}_{GS,t}, d^{up}_{LS,t}, d^{dn}_{LS,t}, d^{1,up}_{GD,t}, d^{1,dn}_{GD,t}, d^{2,up}_{GD,t}, d^{2,dn}_{GD,t}],\end{aligned}$$

where the up and dn superscripts represent the upward and downward reserve capacity from generators and loads to account for under- and over-forecasting of wind power. The operating time horizon is discretized into $T = 24$ time intervals, each having the length $\Delta\tau = 1$ hour, and represented by the indices $t = 1, \ldots, T$. The operational cost is then defined as:

$$\begin{aligned} F(\{x_t\}_{t=1}^T) = &\sum_{t=1}^{T} C_n(P_{G,t}) + C_{GS}(R^{up/dn}_{GS,t})\\ &+ C_{LS}(R^{up/dn}_{LS,t}) + C_{GD}(R^{up/dn}_{GD,t})\end{aligned}$$

where each C represents a cost function. The system constraints include the usual deterministic generation limits, power flow, and power balance constraints, denoted $\mathcal{C}^{\text{det}}$, in addition to (1)-(3), probabilistic constraints associated with the secondary reserves and re-dispatch reserves denoted $\mathcal{C}_{LS}$, $\mathcal{C}_{GS}$, and $\mathcal{C}_{GD}$ (with details given in [11]), and energy constraints that check the energy state at the end of the first and last 15 minute-intervals within each hour [11]:

$$0 \leq S_t + (P_{C,t} + R_{LS,t} - P_B(\mathcal{T}_t))\frac{\Delta\tau}{4} \leq \overline{S}(\mathcal{T}_t), \tag{4}$$

$$\begin{aligned} 0 \leq &S_t + (P_{C,t} - P_B(\mathcal{T}_t))\frac{3\Delta\tau}{4}\\ &+ (P_{C,t} + R_{LS,t} - P_B(\mathcal{T}_t))\frac{\Delta\tau}{4} \leq \overline{S}(\mathcal{T}_t),\end{aligned} \tag{5}$$

$$\begin{aligned} 0 \leq &S_t + (P_{C,t} - P_B(\mathcal{T}_t))\frac{3\Delta\tau}{4}\\ &+ (P_{C,t} + R_{LS,t} - P_B(\mathcal{T}_t))\frac{\Delta\tau}{4} \leq \overline{S}(\mathcal{T}_{t+1}).\end{aligned} \tag{6}$$

for $t = 1, \ldots, T$, where $R_{LS,t}$ is the actual controllable load secondary reserves deployed. We denote (4)-(6) as $\mathcal{C}^{\text{load}}_{\text{dyn}}$.

Finally, the optimal day-ahead dispatch is:

$$\begin{aligned} \text{minimize}_{\{x_t\}_{t=1}^T} \; & F\left(\{x_t\}_{t=1}^T\right)\\ \text{subject to} \quad & \mathcal{C}^{\text{det}}\\ & \mathbb{P}\left(\mathcal{C}_{LS} \cap \mathcal{C}_{GS} \cap \mathcal{C}_{GD} \cap \mathcal{C}^{\text{load}}_{\text{dyn}}\right) \geq 1 - \epsilon\end{aligned}$$

where the stochastic constraints are required to meet the specified probability level $1-\epsilon$ jointly. It is also possible to write individual chance constraints, where each stochastic constraint i is required to meet a specified probability level $1 - \epsilon_i$ individually. In the latter case, different ϵ_i can be selected for each constraints allowing critical constraints or time periods to be managed in a robust way, with increased flexibility elsewhere.

D. Representing Wind Uncertainty

One of the main challenges in integrating weather-dependent sources of power, such as wind, is the variable and intermittent nature of the power source. For example, in the particular case of wind generation, the complex behavior of this resource is exacerbated by non-linear interactions between the turbines and highly variable wind speeds, which in turn create significant technical difficulties in providing a complete characterization of its temporal and spatial dynamics. As a result, improvement in wind power forecasting accuracy is acknowledged as a critical need for a secure and reliable operation of the power system [19]–[21]. Current approaches addressed in the literature include weather prediction models [22] and stochastic process models [23]–[25]. The interested reader is referred to [24] for a review on existing developments in this area.

Actual forecast data is proprietary, and twenty-four hour forecast trajectories were not available for this study. In order to implement the stochastic model described in Section II, wind farms were based on the NREL-Eastern Wind Integration Study dataset [26], which provides synthetic wind farm output data for a large number of locations across the eastern region of the United States. For this study, four wind farms were placed in the IEEE 30-bus network, as shown in Table I.

Bus	1	10	20	30
Capacity (MW)	400	460	631	652

Table I: Wind Generation Capacity.

The data used for these simulations are selected to represent 24-hour trajectories with similar wind temporal patterns originating from a similar initial condition (wind level). Using three years of synthetic data, clustering analysis yielded 54 similar trajectories of data. Wind capacities were scaled to achieve the desired penetration of wind power in the network. A single representative trajectory was selected to represent a daily forecast for each location, with the remaining trajectories used to represent wind scenarios and estimate a distribution of forecast errors, as described in [27]. Figure 1 illustrates the aggregated wind power scenarios used in our numerical instances presented in Section III.

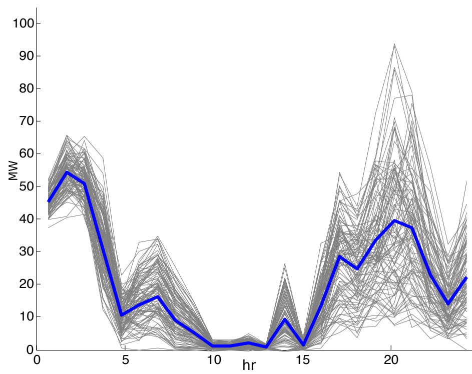

Figure 1: Aggregated wind power forecast (blue) and scenarios (grey).

III. Numerical Results

In this section, the robust-scenario approach developed by [28] and used in [9], [11] and the percentile approach of [10] are used to compare risk-averse solutions representing different reliability requirement levels.

A. Test Setting

The setup of the system considered in the test case is as follows: the IEEE 30-bus system is modified to include four wind farms located at buses 1, 10, 20, and 30 to achieve a maximum wind penetration level corresponding to 30% of the total system load. We used a sufficiently large set of scenarios ($\simeq$10000) to ensure the robustness of the. The physical properties of the conventional units and their cost of generation were modeled as in [29, case30]. The temperature profile used in this study corresponds to an average summer day in the state of New York (see Fig. 2, top), and it is assumed that 10% of each load in the system is controllable. The controllable portion of the load is modeled as an aggregation of AC units such that at higher temperatures the AC units need to provide more cooling and thus draw more power. The power and energy capacity of an aggregation of AC units is shown in Fig. 2 (middle/bottom).

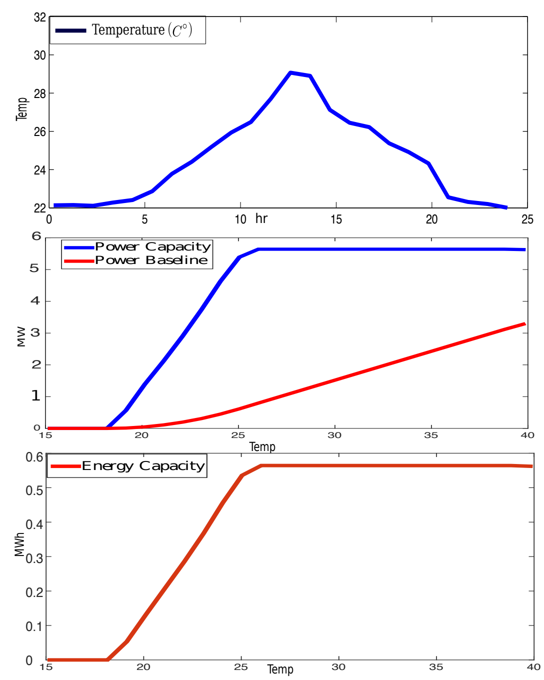

Figure 2: Temperature profile (top); Power capacity and power baseline (in MW) as a function of temperature for an aggregation of 1000 air conditioners (middle); and energy capacity (in MWh) as a function of temperature for an aggregation of 1000 air conditioners.

The reserve cost functions are assumed linear in the reserve capacity and specified in \$/MW. The cost of reserves from generators was set as shown in Table II, where c_{GS} and c_{GD} represent secondary and re-dispatch reserve costs, respectively, and upward and downward capacity are assumed to be equivalent in cost. The cost of secondary reserves are set higher than the cost of re-dispatch reserves because secondary reserves are faster responding.

The cost of load reserves is lower than both types of

Generators	1	2	3	4	5	6
c_{GS}	6	6.75	7	5.25	5	5
c_{GD}	2.4	2.1	1.2	3.9	2	3.6

Table II: Generator Reserve Costs

generator reserves and time dependent, as follows:

$$c_{LS,t} = 1.1 - \tilde{S}(\mathcal{T}_t), \tag{8}$$

where $\tilde{S}(\mathcal{T}_t)$ is the energy capacity of the controllable loads normalized by the maximum hourly load and the upward and downward capacity are again assumed equivalent in cost.

In this analysis, three risk-averse approaches were considered to manage uncertainty introduced through wind forecast error, including i) a *robust* approach where the solution seeks to protect against all possible forecast errors, ii) *percentile* approach where the model requires protection against the 90% probability level of deviations, iii) *percentile-robust* or hybrid approach where robustness is required at times of greatest uncertainty, while probabilistic protection is sought for periods of time where errors are within a prescribed tolerance, and therefore considered less critical. Specifically, in i) we generate 10,000 wind forecast error scenarios from the distributions described in Section II.D and use the approach of [28] to formulate a probabilistically robust problem. In ii), we use the percentile approach of [10], in which the scenarios are ordered and the problem is solved to ensure all scenarios within the 90th percentile are satisfied. In iii), we use the robust approach at critical times (i.e., all constraints corresponding to those times must be satisfied in all 10,000 scenarios) and the percentile approach at other times (i.e., all constraints corresponding to other times must be satisfied for only 90% of the scenarios). In this mixed approach, critical times are defined as those hours where the wind forecast errors are particularly high (RMS > 0.7).

Numerical simulations were implemented in MATLAB and the optimization problem was solved using the Gurobi solver Version 6.0.4.

B. Results

As shown in Fig. 3, there are small differences in the reserves provided by the controllable portion of the loads under different reliability requirement levels. In Fig. 3, markers represent the controllable load set point computed with the wind power forecast, and the corresponding bars indicate the load reserve scheduled at each period of time. Due to limitations on the energy state of the controllable loads and the low cost of load reserves, the system always prefers to dispatch reserves from the loads, and nearly universally allocates all available reserves from controllable loads. As a result, the allocation of load-based reserves are not particularly sensitive to variations in imposed reliability requirements.

Figure 4 illustrates the reserve schedules at different reliability levels. From this figure, it is clear that a robust approach requires more reserves, as the system prepares to accommodate the maximum forecast errors at all times. A disadvantage of the robust approach is that the solution is also likely to stress the generating units under high wind penetration levels. For example, Fig. 5 plots the secondary and re-dispatch reserves of the generator at bus 23 (unit 5), with the markers representing the power dispatch computed with the wind power forecast, and the bars showing the amount of reserve the unit is required to provide at each period of time. The robust approach tends to allow drastic variations of its power output which could lead to infeasibilities when ramping is considered in the model. The percentile and percentile-robust policies reduce these possible drastic power-output variations; therefore, these types of approaches could more effectively incorporate ramping in the model. According to the reliability level, a wind power curtailment policy could also be computed.

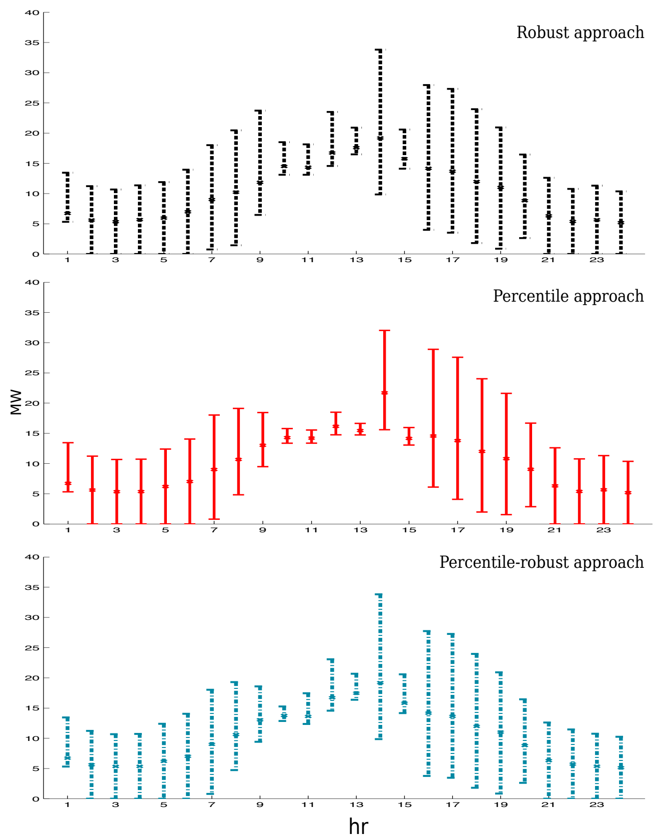

Figure 3: Secondary reserves provided by *loads* show only slight differences among reliability requirements.

Finally, the re-dispatch and secondary reserves of the system are presented in Fig. 6. In general, the robust approach schedules larger amounts of reserves when compared to the other approaches. An in-depth analysis of the generating reserve requirements of each generator would assist in analysis of the effects of each approach.

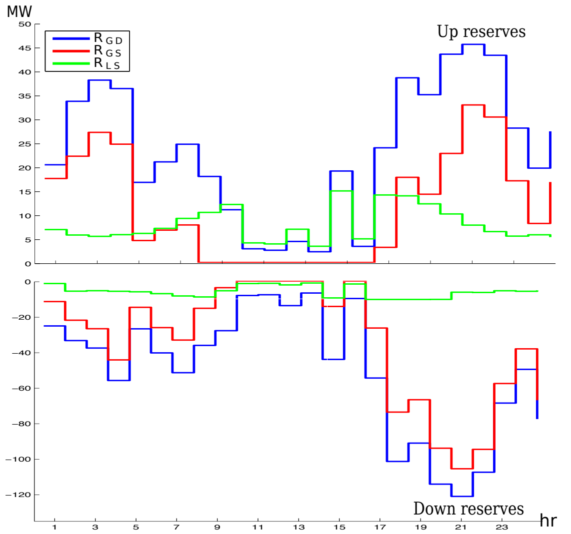

(a) Reserves with robust approach

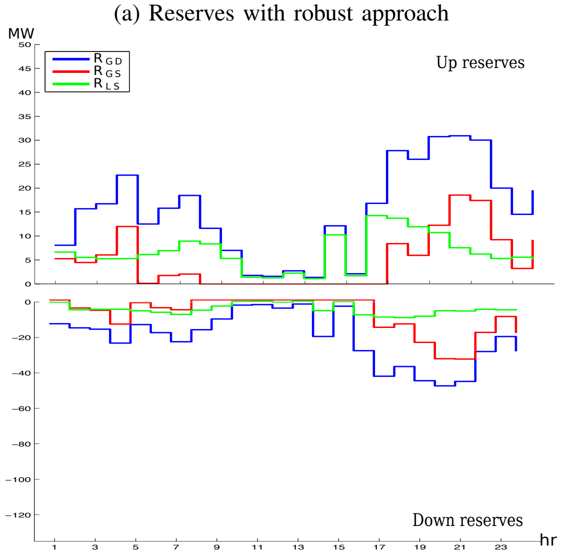

(b) Reserves with percentile approach

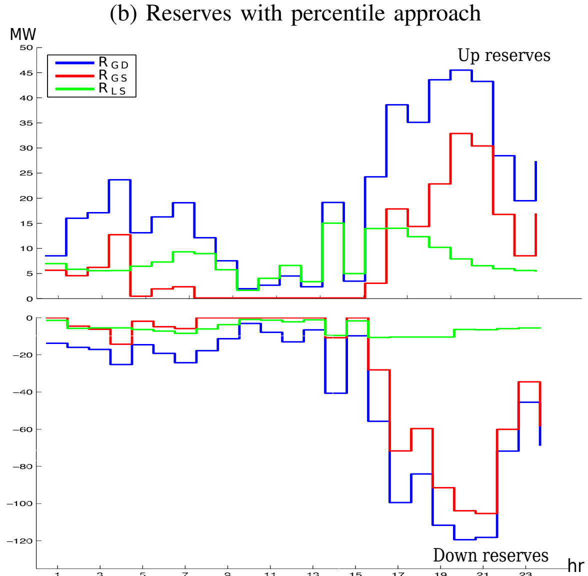

(c) Reserves with percentile-robust approach

Figure 4: Comparison of reserve allocation.

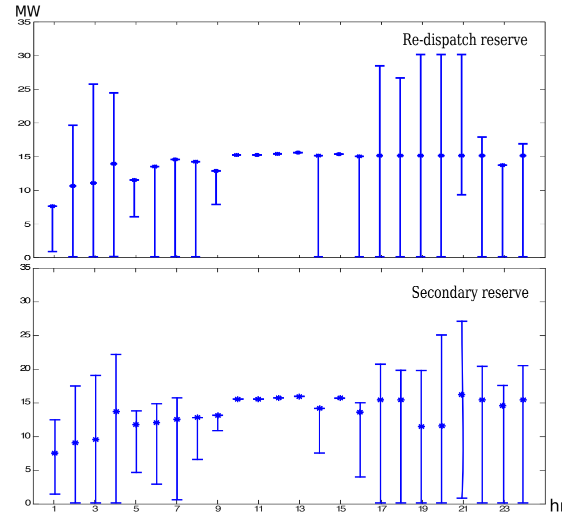

(a) Reserves with robust approach

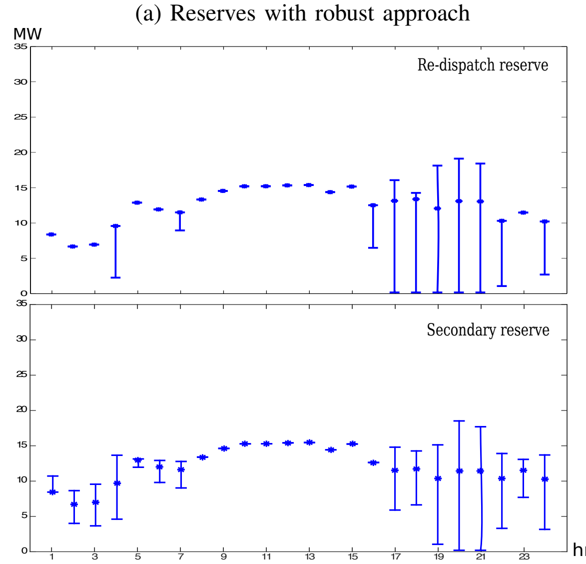

(b) Reserves with percentile approach

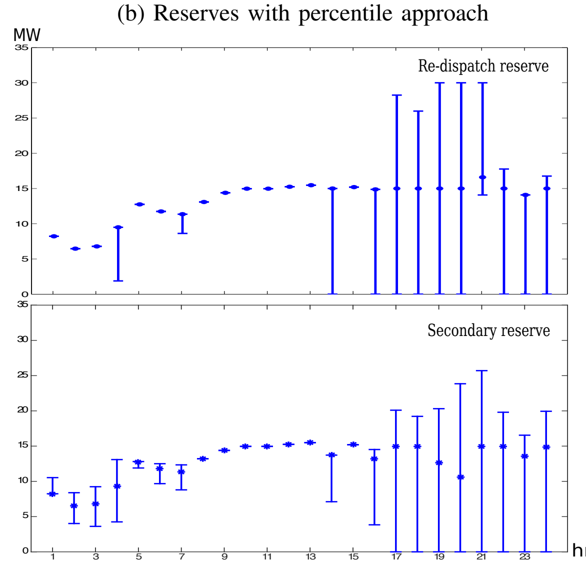

(c) Reserves with percentile-robust approach

Figure 5: Comparison of secondary and re-dispatch reserves of unit 5, bus 23.

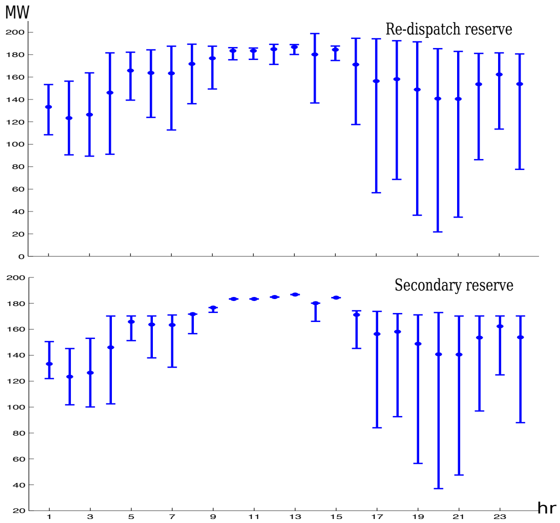

(a) Reserves with robust approach

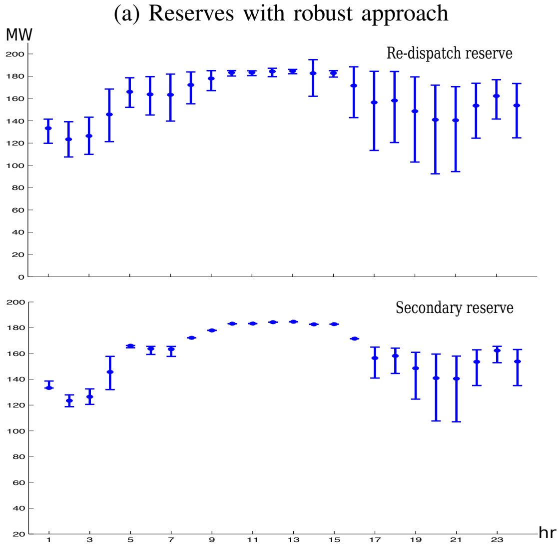

(b) Reserves with percentile approach

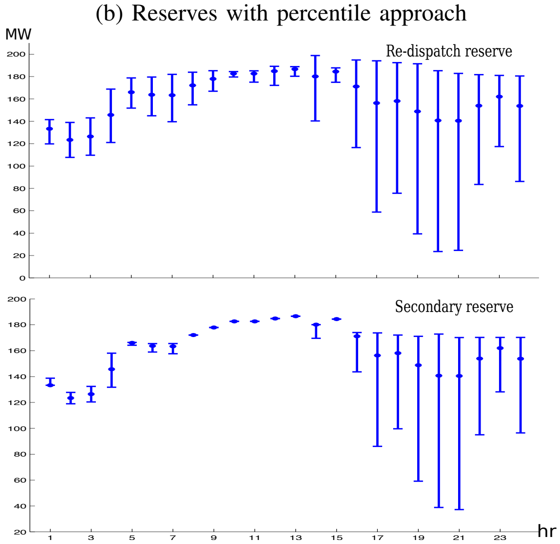

(c) Reserves with percentile-robust approach

Figure 6: Comparison of secondary and re-dispatch reserve of the system.

IV. Concluding Remarks

This paper presents a simulation-based analysis comparing robust, percentile, and percentile-robust approaches to explore the balance between reliability and reserve requirements. While the robust approach is more risk-averse and allocates more generating and load reserves, the solution shows significant variance in reserve requirements throughout the operating horizon, which will likely lead to unnecessary stress for the conventional generating units at high penetration levels of wind power. Conversely, the percentile approach allows some reduction in reserve requirements, and the percentile-robust approach could further ensure more robust allocations at critical times. That is likely to be a beneficial balance for the system as more flexible policies will be needed to incorporate ramping constraints and accommodate different importance levels at different times of day and locations on the network.

Future directions will include the investigation of the impact of ramping constraints in the model, as it is hypothesized that some reserve allocations will result in infeasbilities, particularly in the robust case. In addition to ramping, implementing unit commitment (UC) is a crucial step to determine a cost-effective day-ahead planning of the system. This model can be extended by incorporating the UC approach presented in [10]. Finally, the work presented here does not include potential curtailment of wind resources, and this strategy is worth examining in future implementations of the model.

References

[1] C. Murillo-Sanchez, R. Zimmerman, C. Anderson, and R. Thomas, "A stochastic, contingency-based security-constrained optimal power flow for the procurement of energy and distributed reserve," *Decision Support Systems*, vol. 56, pp. 1–12, May 2013.

[2] A. Papavasiliou, S. Oren, and R. O'Neill, "Reserve Requirements for Wind Power Integration: A Scenario-Based Stochastic Programming Framework," *Power Systems, IEEE Transactions on*, vol. 26, no. 4, pp. 2197–2206, November 2011.

[3] J.-P. Watson, S. M. Ryan, and D. L. Woodruff, "Stochastic Unit Commitment: Scalable Computation and Experimental Results," in *FERC Staff Technical Conference on Increasing Real-Time and Day-Ahead Market Efficiency through Improved Software*, Washington DC, Jun. 2013.

[4] D. Bertsimas, E. Litvinov, A. Sun, J. Zhao, and T. Zheng, "Adaptive Robust Optimization for the Security Constrained Unit Commitment Problem," *IEEE Transactions on Power Systems*, vol. 28, no. 1, pp. 52–63, 2013.

[5] R. Jiang, J. Wang, and Y. Guan, "Robust Unit Commitment With Wind Power and Pumped Storage Hydro," *Power Systems, IEEE Transactions on*, vol. 27, no. 2, pp. 800–810, june 2015.

[6] A. Lorca and A. Sun, “Adaptive Robust Optimization With Dynamic Uncertainty Sets for Multi-Period Economic Dispatch Under Significant Wind,” *Power Systems, IEEE Transactions on*, pp. 1–12, june 2015.

[7] W. Wu, J. Chen, B. Zhang, and H. Sun, “A Robust Wind Power Optimization Method for Look-Ahead Power Dispatch,” *IEEE Transactions on Sustainable Energy*, vol. 5, no. 2, pp. 507–515, April 2014.

[8] D. Bienstock, M. Chertkov, and S. Harnett, “Chance-Constrained Optimal Power Flow: Risk-Aware Network Control under Uncertainty,” *SIAM Review*, vol. 56, no. 3, pp. 461–495, Aug. 2014.

[9] M. Vrakopoulou, K. Margellos, J. Lygeros, and G. Andersson, “A probabilistic framework for reserve scheduling and N-1 security assessment of systems with high wind power penetration,” *IEEE Transactions on Power Systems*, vol. 28, no. 4, 2013.

[10] G. Martinez and C. L. Anderson, “A Risk-averse Optimization Model for Unit Commitment Problems,” *Proceedings of the 48th Hawaii Conference on System Sciences*, pp. 1–9, 2015.

[11] M. Vrakopoulou, J. Mathieu, and G. Andersson, “Stochastic Optimal Power Flow with Uncertain Reserves from Demand Response,” in *Hawaii International Conference on System Sciences (HICSS)*. IEEE, 2014, pp. 2353–2362.

[12] B. Li and J. Mathieu, “Analytical Reformulation of Chance-Constrained Optimal Power Flow with Uncertain Load Control,” in *PowerTech*, 2015, pp. 1–6.

[13] A. Lamadrid, T. Mount, R. Zimmerman, C. Murillo-Sanchez, and C. L. Anderson, “Alternate mechanisms for integrating renewable sources of energy into electricity markets,” *IEEE Power and Energy Society General Meeting*, June 2012.

[14] A. M. Gopstein, “Energy Storage and the Grid - From Characteristics to Impact [Point of View],” *Proceedings of the IEEE*, vol. 100, no. 2, pp. 311–316, June 2015.

[15] J. Cardell and C. L. Anderson, “A Flexible Dispatch Margin for Wind Integration,” *IEEE Transactions on Power Systems*, pp. 1–8, May 2014.

[16] M. Ilic, L. Xie, and J. Joo, “Efficient Coordination of Wind Power and Price-Responsive Demand, Part I: Theoretical Foundations,” *Power Systems, IEEE Transactions on*, vol. 26, no. 4, pp. 1875–1884, June 2011.

[17] D. Callaway and I. A. Hiskens, “Achieving Controllability of Electric Loads,” *Proceedings of the IEEE*, vol. 99, no. 1, pp. 184–199, June 2015.

[18] J. Mathieu, M. Kamgarpour, J. Lygeros, G. Andersson, and D. Callaway, “Arbitraging intraday wholesale energy market prices with aggregations of thermostatic loads,” *IEEE Trans Power Systems*, vol. 30, no. 2, pp. 763–772, 2015.

[19] D. Lew, M. Milliga, G. Jordan, and R. Piwko, “The value of wind power forecasting,” National Renewable Energy Laboratory, Tech. Rep. NREL/CP-5500-50814, January 2011.

[20] S. Soman, H. Zareipour, O. Malik, and P. Mandal, “A review of wind power and wind speed forecasting methods with different time horizons,” in *North American Power Symposium (NAPS), 2010*, Sept 2010, pp. 1–8.

[21] A. Foley, P. Leahy, A. Marvuglia, and E. McKeogh, “Current methods and advances in forecasting of wind power generation,” *Renewable Energy*, vol. 37, no. 1, pp. 1–8, 2012.

[22] M. Marquis, J. Wilczak, M. Ahlstrom, J. Sharp, A. Stern, J. Smith, and S. Calvert, “Forecasting the wind to reach significant penetration levels of wind energy,” *Bulletin of the American Meteorological Society*, vol. 92, no. 9, pp. 1159–1171, 2011.

[23] M. Lange, “On the uncertainty of wind power predictions—analysis of the forecast accuracy and statistical distribution of errors,” *ASME. J. Sol. Energy Eng*, vol. 127, pp. 177– 184, 2005.

[24] P. Pinson, “Wind energy: Forecasting challenges for its operational management,” *Statistical Science*, vol. 28, no. 4, pp. 564–585, 11 2013.

[25] B. Hodge and M. Milligan, “Wind power forecasting error distributions over multiple timescales,” *Power and Energy Society General Meeting, 2011 IEEE*, pp. 1–8, 2011.

[26] NREL, “Wind systems integration eastern wind integration and transmission study,” National Renewable Energy Laboratory, Tech. Rep., 2010.

[27] C. L. Anderson and R. D. Zimmerman, “Wind Output Forecasts and Scenario Analysis for Stochastic Multiperiod Optimal Power Flow,” in *PSERC Webinar*, Mar. 2011, pp. 1–38.

[28] K. Margellos, P. Goulart, and J. Lygeros, “On the road between robust optimization and the scenario approach for chance constrained optimization problems,” *IEEE Transactions on Automatic Control*, vol. 59, no. 8, pp. 2258–2263, 2014.

[29] R. Zimmerman, C. Murillo-Sanchez, and R. Thomas, “Matpower’s extensible optimal power flow architecture,” in *Power Energy Society General Meeting, 2009. PES ’09. IEEE*, July 2009, pp. 1–7.